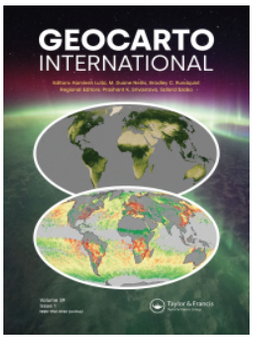

Geocarto International

ISSN: 1010-6049 (Print) 1752-0762 (Online) Journal homepage: www.tandfonline.com/journals/tgei20

Evaluation of global remotely sensed evapotranspiration products in arid irrigated agricultural environments using ground measurements

Phathutshedzo Eugene Ratshiedana, Mohamed A. M. Abd Elbasit, Elhadi Adam & Johannes George Chirima

To cite this article: Phathutshedzo Eugene Ratshiedana, Mohamed A. M. Abd Elbasit, Elhadi Adam & Johannes George Chirima (2025) Evaluation of global remotely sensed evapotranspiration products in arid irrigated agricultural environments using ground measurements, Geocarto International, 40:1, 2528555, DOI: 10.1080/10106049.2025.2528555

To link to this article: https://doi.org/10.1080/10106049.2025.2528555

Published online: 08 Jul 2025.

GEOCARTO INTERNATIONAL
2025, VOL. 40, NO. 1, 2528555
https://doi.org/10.1080/10106049.2025.2528555

Taylor & Francis
Taylor & Francis Group

Evaluation of global remotely sensed evapotranspiration products in arid irrigated agricultural environments using ground measurements

Phathutshedzo Eugene Ratshiedana[a,b], Mohamed A. M. Abd Elbasit[c], Elhadi Adam[a] and Johannes George Chirima[b,d]

[a]School of Geography, Archaeology and Environmental Studies, University of the Witwatersrand, Wits, Johannesburg, South Africa; [b]Agricultural Research Council-Natural Resources and Engineering-Geoinformatics, Arcadia, Pretoria, South Africa; [c]Department of Physical and Earth Sciences, School of Natural and Applied Sciences, Arid Region Water Research Centre, Sol Plaatje University, Kimberley, South Africa; [d]Department of Geography, Geoinformatics and Meteorology, University of Pretoria, Pretoria, South Africa

ABSTRACT

Accurate quantification of crop water requirement is essential for efficient irrigation practices. However, direct measurement of crop water use is localised and impractical over large areas. Remotely sensed evapotranspiration (ET) provides a solution by estimating spatial explicit ET. Nevertheless, the accuracy of ET products in South African irrigated agriculture remains uncertain. This study evaluated the accuracy of MODerate Resolution Imaging Spectroradiometer (MOD16), Noah Land Surface Model Evapotranspiration Product (NOAH) and Water Productivity Open-access Portal (WaPOR) products retrieved using Google Earth Engine (GEE). A stepwise validation approach was applied integrating lysimeter-derived actual evapotranspiration (ETa) with reference evapotranspiration (ETo) to extrapolate ETa across the Vaalharts irrigation scheme. Results demonstrated WaPOR as a promising product with correlations of 0.69 to 0.88, and lower errors with RMSE from 0.87 to 3.22 mm d^{-1}, while MOD16 and NOAH estimates are poor. These findings demonstrate WaPOR as a potential tool for improving irrigation water management.

ARTICLE HISTORY
Received 2 December 2024
Accepted 29 June 2025

KEYWORDS
Actual evapotranspiration; WaPOR; MOD16; NOAH; smart field weighing lysimeter

1. Introduction

Actual evapotranspiration (ETa) in agriculture is regarded a crucial hydrological component used to determine the actual amount of water lost after known amounts of irrigation or rainfall (Djaman et al. 2018). This component defines the actual amount of water lost through transpiration and soil water evaporation after irrigation or rainfall (Gutry-Korycka 2019). This parameter is key for ensuring that there is a balance

CONTACT Phathutshedzo Eugene Ratshiedana ratshiedanap@arc.agric.za

between water inputs and water that has been lost from a cropped surface (Bodner et al. 2015). By quantifying ETa, it is possible for farmers to apply a precise amount of water as irrigation. This benefits farmers in reducing the costs associated with irrigation water supplies while also reducing the overuse of water, this ensures that water resources are conserved while crops develop and produce optimally (Zhang and Long 2021; Abbasi et al. 2023).

Irrigated agriculture is the largest consumer of global freshwater resources estimated to use more than 70% of the available amounts (Ingrao et al. 2023). However, there is a lack of precise methods for determining the optimal crop water usage in agriculture which leads to inefficient irrigation practices. Gleick (2023) suggested that the issue is not often with the water supply but with how it is used during irrigation. In the absence of ETa data, farmers are bound to use more water than what crops require resulting in greater water losses through ETa (Djaman et al. 2018). In South African regions where most arid conditions prevail, agriculture accounts for approximately 70% of freshwater usage through irrigation; this percentage is more likely to increase as climate change impacts intensify and water competition increases (Du Plessis 2019).

Efforts by the departments of water and sanitation, agriculture and forestry are underway to better manage agricultural water consumption, yet accurate ground-based measurement methods to quantify ETa in South Africa remain limited. The Department of Water Affairs (DWA) in South Africa advocates for advanced satellite data to improve the monitoring of irrigated areas and water usage (DWS 2006). However, challenges persist because of limited site-specific data for the calibration of satellite estimates which further complicates irrigation scheduling (Gibson et al. 2013; Ramoelo et al. 2014). The fact that ETa reflects water loss through evaporation and plant transpiration, it becomes key for monitoring crop water use effectively (Gutry-Korycka 2019).

Conventional ETa measurement methods, which include the use of eddy covariance systems and lysimeters offer high-accuracy ETa at field scales but typically lack the capacity to cover large, heterogeneous landscapes cost-effectively (Khan et al. 2020; Elfarkh et al. 2022). This is because direct measurement devices are expensive, making them impractical for deployment across vast landscapes. Satellite-based remote-sensing approaches can address these spatial limitations at lower costs and with increased accessibility through platforms such as the Google Earth Engine. Despite these advances, limitations remain in terms of spatial and temporal resolutions (Khanal et al. 2020). To facilitate effective global water management, several ETa satellite products are available, including MOD16, WaPOR, NOAH and Global Land Evaporation Amsterdam Model (GLEAM), which are derived though different algorithms. These products were developed in temperate regions and may not accurately represent South Africa's diverse conditions. The validation and calibration of these products is essential in the Southern Hemisphere, where ground validation data is limited. However, in South Africa, MOD16 and several products have shown mixed reliability when tested against measured data from devices such as eddy covariance towers and climate data (Ramoelo et al. 2014; Jovanovic et al. 2015).

Given the significant role of evapotranspiration (ET) in the hydrological cycle and its impact on the environment as a system, several studies have been undertaken to assess the accuracy of remotely sensed ET products estimated by different algorithms and models at diverse levels. For example, in South Africa, Ramoelo et al. (2014) evaluated the accuracy of the MOD16 global ET product, which was generated from the Penman-Monteith algorithm using two eddy covariance flux towers in the woodland environment of Kruger Park in northern South Africa. They reported inconsistent correlations among the MOD16 ET estimations and flux tower ET measurements, which they concluded that the inconsistencies might have been a result of the parameterization of the deriving algorithm or associated with errors in the flux tower measurement. In another study, Jovanovic et al. (2015) presented a national–scale validation of the MOD16 ET product in South Africa using meteorological data. They reported that the MOD16 ET product underestimated ET estimates by 15%. These findings provide an opportunity to assess, improve and review algorithms for ET estimation at different scales using improved devices and approaches in South Africa. Majozi et al. (2017) assessed the accuracy of two global ET products, MOD16 and GLEAM, in two different ecosystems using a scintillometer and an eddy covariance flux tower in two semi-arid environments. They reported variations in accuracy between measured and global ET from both assessment sites. Another study was undertaken by Ndara (2017), who analysed monthly MOD16 ET fluxes at two sites with varying climatic conditions in South Africa. A scintillometer was used to validate MO16 ET fluxes in a humid environment, whereas eddy covariance systems were used to validate ET in semiarid environments. Ndara (2017) reported that the average ET derived from a scintillometer varied from the average MOD16 ET, whereas there was no significant difference in the average ET obtained using the eddy covariance and MOD16. The evaluation of WaPOR in South Africa has been done using flux towers belonging to FLUXNET in non-agricultural environments in a continental-level study (Blatchford et al. 2020). However, the evaluation of the product in agricultural environments has not been conducted against accurate measurements. Furthermore, less to no attention has been given to the use of weighing lysimeters for the determination of actual ET. Validation of global ET products within agricultural environments is crucial for understanding their application in agricultural irrigation water management. The greatest challenge in South Africa for validating these products in agricultural environments is the availability of ET measuring devices.

Although the greatest challenge has been direct ET measurements, the Food and Agriculture Organization (FAO) developed an approach to estimate crop evapotranspiration (ETc) using reference evapotranspiration (ETo) with crop coefficient (Kc) values to estimate crop evapotranspiration (ETc) using published Kc values (Allen et al. 1998). The limitation of this approach its demand for local Kc adjustments for accurate irrigation scheduling, this is often limited by the demand to ETa to derive Kc values. The ETo component defines the atmospheric water demand as opposed to ETa (Allen et al. 1998). The Penman-Monteith model is the standard for ETo estimation but requires extensive data, which may not always be available. In such cases, alternative models using limited inputs are applied. Bashir et al. (2023) proposed the use of machine learning to address this issue. On follow-up, Bashir et al. (2024)

found Light Gradient Boosting Machine Regressor (LightGBMR) being the most accurate machine learning approach of various algorithms tested in estimating ETo. Ratshiedana et al. (2025) made highlights on the importance of accurate ETo data in scaling ETa from field-scale to regional levels using meteorological stations and modelling approaches.

Climate change is intensifying water scarcity and altering crop water requirements which is posing a major challenge for sustainable agriculture. Studies indicate that future irrigation water requirements will increase significantly, requiring advanced monitoring and adaptive water management strategies (Gabr 2022). In arid regions, precision irrigation informed by high-accuracy ETa estimates is crucial to ensuring crop productivity while minimizing water wastage (Zhang and Long 2021). Therefore, accurate ETa estimation contributes to several United Nations Sustainable Development Goals (SDGs), firstly, ETa contributes to SDG 2 on zero hunger directly influencing crop growth and productivity. Secondly it contributes to SDG 6 on clean water and sanitation, quantifying ETa accurately reduces the overuse of water while availing water for other current and future uses. Lastly, ETa contributes to SDG 13 on climate action by promoting sustainable water management, ensuring resilience in agriculture and ecosystems under changing climate conditions (Gabr et al. 2024). The current study aimed to bridge the existing ETa data gaps in irrigated agricultural environments by integrating accurate ETa data measurements from a smart field weighing lysimeter with meteorological data from weather stations within the Vaalharts irrigation scheme in South Africa. The primary objective of this study was to evaluate the accuracy and reliability of MOD16, NOAH and WaPOR ETa products for agricultural water use monitoring and management. To achieve this, a stepwise validation approach was used extrapolating lysimeter-derived ETa data across multiple weather stations. This is because more weather stations exist in most areas compared to lysimeters. Satellite estimated ETa products were retrieved using GEE platform for comparison with ground-observations. Statistical metrics were used to assess the accuracy of the three different products. A multi-source validation framework which systematically evaluates the performance of remotely sensed ETa estimates across different temporal and spatial scales was developed. Using this approach improves the scalability of ETa estimates while adding more insights on the uncertainties of different remote sensing ETa products which can improve irrigation planning and water management in water-scarce regions significantly.

2. Materials and methods

2.1. Study area description

The study was conducted at different parts of the Vaalharts irrigation scheme which is situated within the Northern Cape Province in South Africa (Figure 1). The scheme is a major hub for most crops and is well known for pecan production (Maisela 2007). The central coordinates of the Vaalharts are 28°06′56.84″ S and 24°55′32.50″ E. The Vaalharts irrigation scheme is the largest irrigation scheme in South Africa covering more than 369.50 km^2 (Ratshiedana et al. 2023). The Vaalharts irrigation scheme is located between two plateaus, while it has nearly flat terrain with elevations

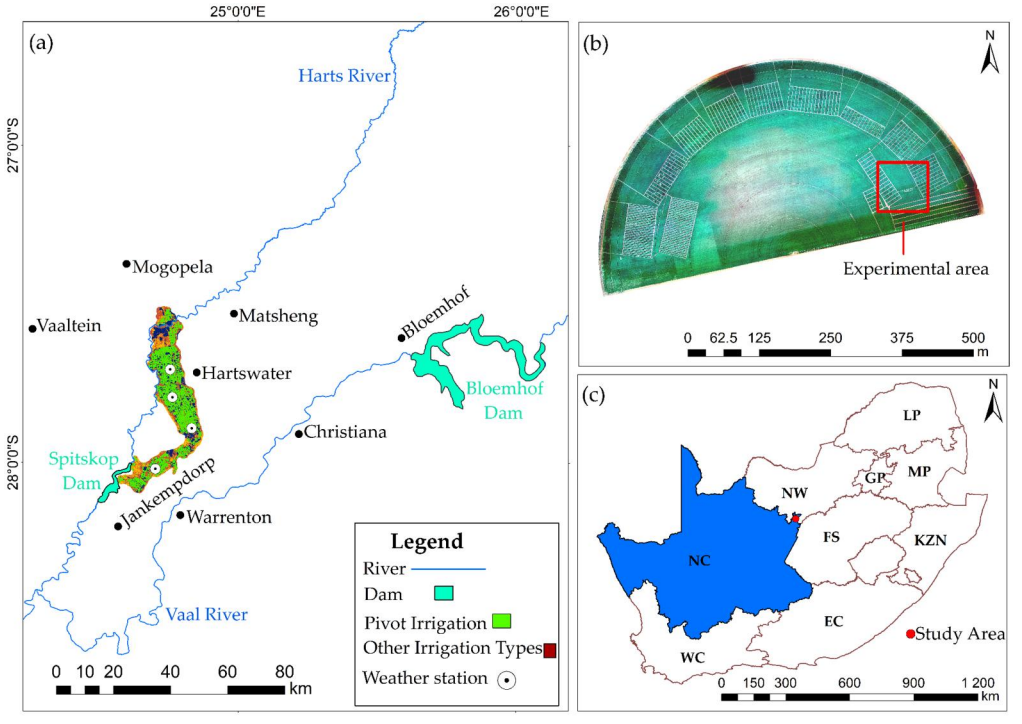

Figure 1. The map depicting the study area's distinct regions: (a) delineates the vaalharts irrigation scheme, (b) identifies the experimental farm, and (c) indicates the study area's position in relation to various South African provinces.

between 1011 and 1192 m above sea level (Verwey and Vermeulen 2011). The Vaalharts irrigation scheme has an annual rainfall less than 400 mm year^{-1} with most rain occurring between late December and late February (Moeletsi et al. 2022). The winter season is cold with a minimum average temperature of 3 °C and the hot summer season has a mean maximum temperature of approximately 43 °C (Moeletsi et al. 2022). The irrigation scheme highly depends on water transfers through canals driving water from the Warrenton weir which accumulates water from the Vaal and Harts Rivers (Maisela 2007). Pivot irrigation systems, drips, furrows, bubblers and sprinklers are used for irrigation (Ratshiedana et al. 2023).

2.2. Lysimeter data collection

Two smart field weighing lysimeters (SFL-600) developed by the METER group© were installed at the experimental farm from 2019 until the 2021 cropping season to measure different components of the water balance at a high temporal resolution of 1-minute intervals (Figure 2). Each lysimeter's inner compartment was a core cylinder of 30 cm in diameter and 60 cm height. Storage variations across seasons were tracked by monitoring changes in the weight of the lysimeter cylinder (Figure 3). Similarly, the drainage component was measured using a separate container resting on its own mass balance. Furthermore, the lysimeter monitored four hydrological factors soil moisture, electrical conductivity, water potential, and soil temperature at depths of 5,

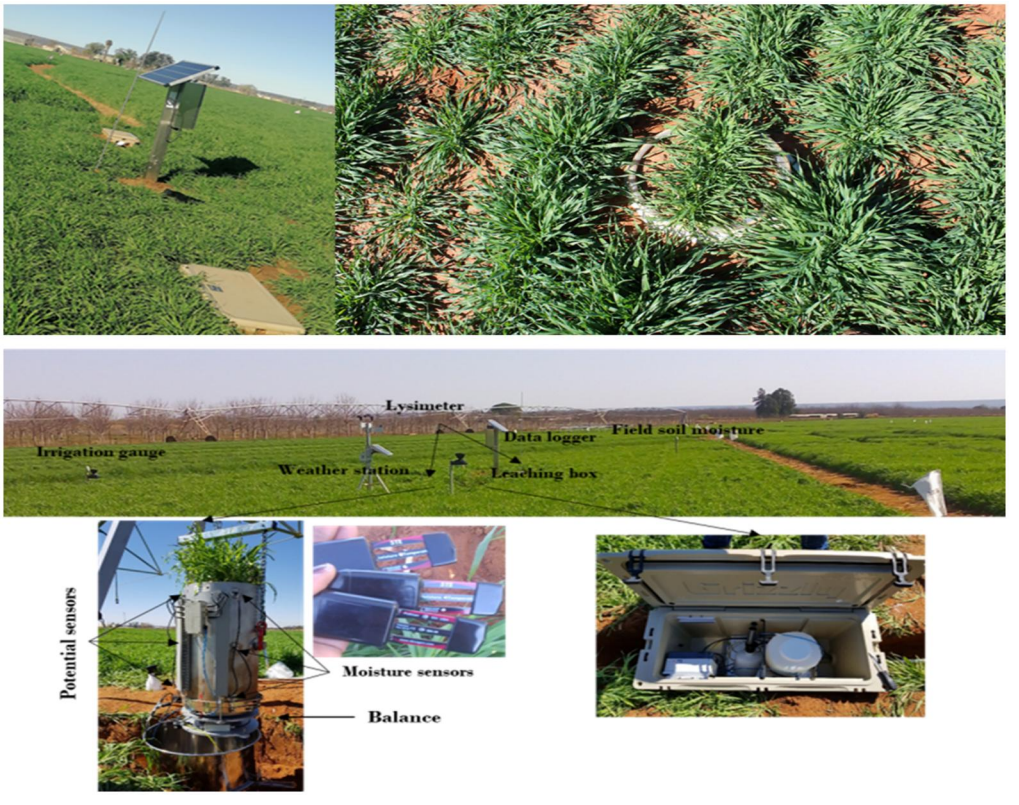

Figure 2. A view of the field experimental setting of the lysimeter and meteorological station.

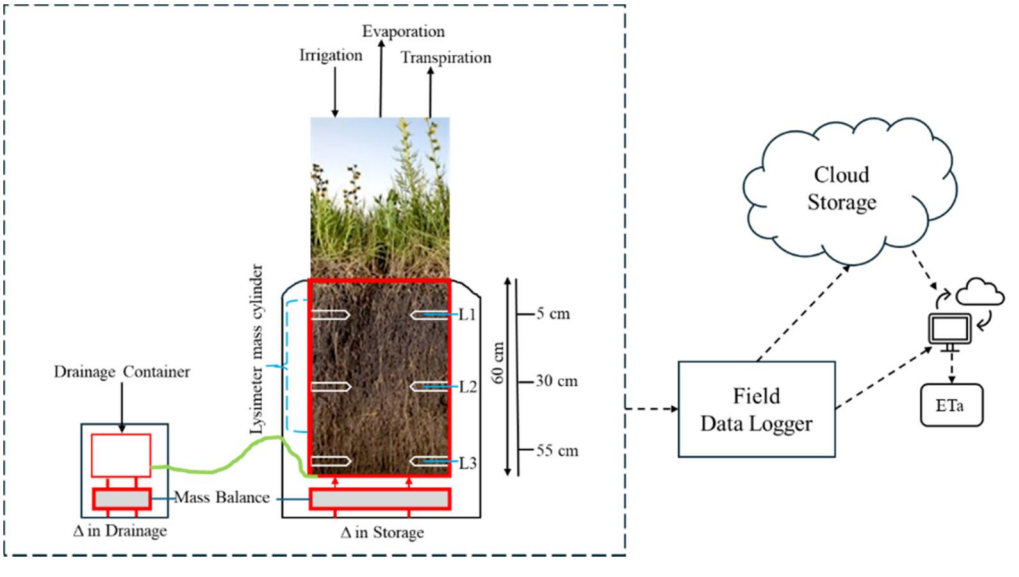

Figure 3. A cross-sectional view of the lysimeter setting at field level.

30, and 55 cm, with readings taken every ten minutes. A field data logger connected to the lysimeter stored all measurements and uploaded them to a cloud storage system, enabling remote access to the data. The lysimeter was reconfigured using the manufacturer's internal calibrations once the installation was completed to ensure accurate measurement, this differs from manual calibration of the weighing balance using known weights. To ensure the lysimeter was accurately measuring the water balance components, a cross-check of the lysimeter mass balance changes with measured irrigation using an external irrigation-gauge was done obtaining no significant variations. The main objective of using the smart field weighing lysimeter was to generate ground truth data to support the validation of MOD16, NOAH and WaPOR ETa products.

2.2.1. Lysimeter data selection and processing for ETa calculations

The lysimeters' instantaneous weight (LYW) and drainage weight (SWW) each season were retrieved from cloud storage for data processing before calculating the ETa fluxes. Due to frequent measurements occurring every minute, both lysimeters' weights contained measurement noise caused by external forces such as wind and vibrations from farm machinery during irrigation, fertigation and fumigation. To remove such noise, the raw data were subjected to Savitzky-Golay filtering using Origin Lab data processing software (Version 10.1.0.170) developed by OriginLab Corporation©. This approach is good for enhancing datasets impacted by random noise (Peters et al. 2014). Moreover, to simplify the quantification of ETa, only days with zero irrigation and zero rainfall were selected for ETa calculations. From the selected data, measurements made between sunrise and sunset were taken. The selection process was essential for aligning the data with calculations based on meteorological datasets, which did not account for nighttime ET. Since the two lysimeters were 10 m apart and giving no significant differences in ETa, average values were used for analysis. The formula for the Savitzky-Golay filter adopted from Peters et al. (2014) can be expressed as follows:

$$y_i = \sum_{j=0}^{N-1} c_j \times x_i + j \tag{1}$$

where y_i is the smoothed value at position i, x_i+j represents the data points within the moving window centred at position i, N is the total number of data points within the window and c_j are the coefficients of the polynomial used for smoothing.

2.2.2. Lysimetric calculation for crop water use quantification

The calculation of ETa was performed using the water balance equation, with particular emphasis on days characterized by the absence of rainfall or irrigation. This approach aimed to isolate and analyse water loss through evaporation from surfaces and transpiration from crops in the absence of external water inputs.

$$P = \ D \ + R + ET + \ \Delta S \tag{2}$$

where P denotes the water input from any external sources of water, such as irrigation or precipitation. D represents the drainage of water into the deep subsurface,

R denotes surface runoff, ET represents the dual process of evaporation and transpiration of water, and ΔS denotes the change in storage.

The fact that water input was excluded in the equation, surface runoff also became negligible, leaving the water balance with three components resulting in the equation being:

$$ET_a = \frac{(LYW_n + SWW_n) - (LYW_{n+b} + SWW_{n+b})}{\left(\frac{\pi}{4}\right)0.3^2} \quad (3)$$

From the given equation, ETa represents the actual evapotranspiration on a n^{th} day, LYWn represents the weight of the lysimeter in kg at midnight on the n^{th} day, and SWWn represents the weight of the percolate water vessel stored in kg at midnight on the n^{th} day. LYWn + b and SWWn + b represent the lysimeter weight and storage vessel weight on the nth day of the next day, respectively.

The water density was assumed to be 1000 kg m^{-3}, while 0.3 was the diameter of the inner core barrel of the lysimeter. To convert the lysimeter mass from kilograms to millimetres, we assumed a water density of 1000 kg m^{-3}, which was subsequently converted to 0.001 m^3. This value of 0.001 m^3 was divided by the surface area of the lysimeter, which was 0.0707 m^2, resulting in a value of 0.014 m, equivalent to 14 mm.

$$ET_{a(24)} = \sum_{i=n}^{23} ETa_i \quad (4)$$

where i represents each hour of the day and ETa_i is the hourly ETa value at hour i.

2.3. Meteorological data collection

Following lysimeter measurements, meteorological data were collected to support the extrapolation of ETa estimates. An automatic weather station (AWS) developed by ONSET-HOBBO© was installed at field level 10 m north of the lysimeter site to measure different meteorological parameters at a height of 2 m (Figure 2). The station measurements were made at 10-minute intervals. Meteorological datasets at different parts of the irrigation scheme were collected using automatic weather stations developed by Campbell Scientific©, this data can be obtained through https://www.arc.agric.za/arc-iscw/Pages/Agrometeorology-Reports.aspx as narrated by Moeletsi et al. (2022). Data from different automatic weather stations was aggregated to match the timescales of satellite ET products being evaluated. There was no missing data in the meteorological dataset used for the evaluation period. The station sensors were regularly calibrated and metadata on sensor drift was incorporated to adjust for instrumental biases. Table 1 shows different weather stations, their locations and codes.

Table 1. Locations and IDs of the meteorological stations used within the scheme.

Station name	ID Code	Type	Longitude (x)	Latitude (y)
SABBI	30985	AWS	24.74339° E	−27.71777° S
Tadcaster	31078	AWS	24.77467° E	−27.82766° S
Jankempdorp	30142	AWS	24.83994° E	−27.95774° S
Ganspan	31079	AWS	24.75651° E	−27.94559° S

Table 2. Overview of the three global remote sensing-based ET products evaluated.

Product	Spatial resolution	Revisit time	Algorithm	Source
NOAH	25°	3 h	Land Surface Model	https://earthengine.google.com/
MOD16	500 m	8-Day	Penman-Monteith	https://earthengine.google.com/
WaPOR	250 m	Dekadal	Penman-Monteith	https://earthengine.google.com/

2.4. Remotely sensed ET product data extraction using google earth engine (GEE)

Three global ET products, MOD 16A2, GLDAS NOAH and WaPOR Version 2 (Table 2), were extracted using GEE, which is a geospatial cloud-based platform for planetary-scale environmental data analysis. To extract the global ET values for the three products across four cropping seasons, the coordinates of weather stations in the Vaalharts irrigation scheme were obtained for use as reference extraction points. The platform was accessed through https://earthengine.google.com/. The station locations and dates ranging between 1st September 2019 and 31st May 2021 were specified on the code editor available in: https://code.earthengine.google.com/. The values of the ET products were saved as .Csv files on Google Drive. A time series ETa data for each product was extracted and analysed for comparison with ground measurements and extrapolated ETa.

2.4.1. Remote sensing for water productivity (WaPOR)

The water productivity open access of remotely sensed derived data (WaPOR) is a global ET product that was developed through a partnership between the Netherlands government and the FAO with a focus on reducing water gaps within the agricultural sector (Blatchford et al. 2020). The product monitors land and crop water productivity while identifying gaps and providing solutions for achieving water use efficiency. This runs on the Penman-Monteith algorithm which offers products at three spatial resolutions: level 1 at 250 m, level 2 at 100 m, and level 3 at 30 m (Blatchford et al. 2020). South Africa is covered by the L1 product (Weerasinghe et al. 2020). The L3 focuses on irrigation schemes and rain-fed areas in Egypt, Ethiopia, Mali and Lebanon (FAO 2019). Although this product provides a finer resolution, it is hampered by its temporal resolution providing ETa estimates of 10-day average. This does not provide immediate solutions in agricultural environments monitoring and making decisions which call for integrating WaPOR data with real-time datasets to provide important information towards water management.

2.4.2. Moderate resolution Imaging Spectroradiometer ET algorithm (MOD16)

MOD16 is a global ET product of the Moderate Resolution Imaging Spectroradiometer instrument aboard the National Aeronautics and Space Administration (NASA) Terra and Aqua satellites launched in 1999 and 2002. The ET product has a 500 m spatial resolution running on an algorithm that is based on the Penman-Monteith model. The model was initially conceived as a single-source model, while some modifications by Mu et al. (2011) expanded its utility. Mu et al. (2011) introduced enhancements, which included considerations for vapor pressure deficit and minimum temperature to constrain stomatal conductance and the use of

the enhanced vegetation index for fractional vegetation cover calculation with a separate computation for soil evaporation. The refinements incorporated the summation of day and night-time ET in the algorithm. A critical limitation of MOD16 product is that it provides an 8-day average of ET. The product often fails to capture short-term fluctuations in ET which can occur due to rainfall, irrigation events or extreme changes in temperature which are often averaged out, this result in a loss of temporal variability. The provision of 8 days ETa often fails to capture short-term water stress, especially in fast-growing crops which require frequent monitoring. Farmers and water managers require near-real-time data for decision making, however MOD16's temporal resolution makes it difficult to respond promptly to drought stress or over-irrigation if used directly. Although such challenges exist, the product is still usable if careful ground measurements of farm and meteorological conditions are accurately measured to support water use monitoring and management.

2.4.3. Global land data Assimilation System's noah ET product

The Global Land Data Assimilation System's (GLDAS) Noah ET product is an advanced tool designed for global-scale monitoring of ETa (Rodell et al. 2004). This product has been crucial for drought monitoring and water management (Qi et al. 2015). The product offers global coverage with a spatial resolution of 28 km, with the model running the captured data every 3 h (Rodell et al. 2004). The high temporal resolution allows detailed observations of daily water cycles and immediate weather impacts. The coarse resolution of Noah product makes it challenging to evaluate based on single validation point requiring multiple sources to provide an averaged effect which is produced when the land cover input layer of GLDAS algorithm averages the vegetation effect.

2.5. Validation process

The validation process followed a stepwise approach (Figure 4), which included the development of an approach to extrapolate ETa data from the field weighing

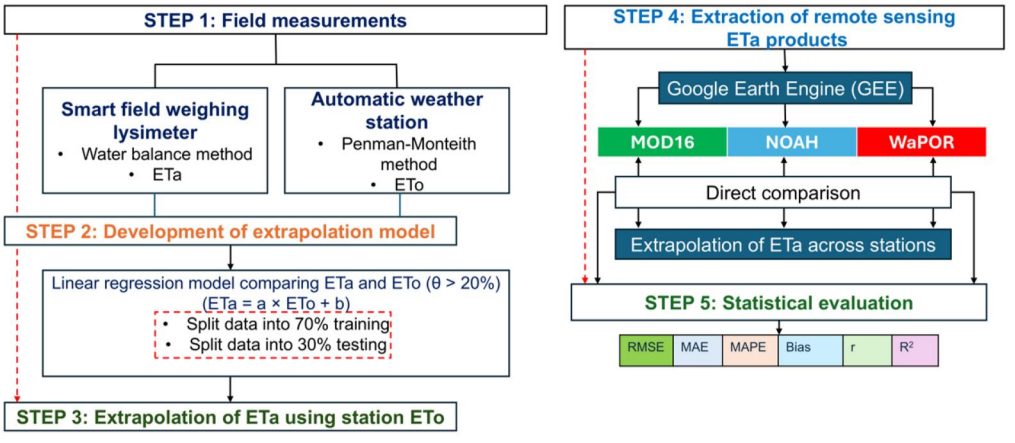

Figure 4. A detailed workflow used for the evaluation of different products.

lysimeter to a nearby weather station that was 10 m north of the lysimeter area. This was necessary for estimating ETa in areas without direct ETa measurement devices. Initially, the data from the lysimeter, which provided high-accuracy ETa measurements, were correlated with the meteorological ETo derived at the weather station under non-stressed soil water condition days. The correlations allowed for the creation of a model that can estimate ETa beyond the lysimeter's immediate location by applying meteorological ETo from any weather station. The stepwise process aimed to establish reliable relationships between direct ETa measurements and ETo to ensure that the extrapolated ETa data remain as accurate as possible even without ground-based ETa instruments across the irrigation scheme. This methodological framework expands the reach of ETa measurements in a cost-effective manner and lays the groundwork for future studies to refine ETa estimation in other agricultural environments with similar direct measurement limitations.

2.5.1. Stepwise validation process

To evaluate the accuracy of various ET products, a multi-step approach was used. This process integrates data from ground-based lysimeters and automatic weather stations with the standard global ETo model (Penman-Monteith).

Step 1. Lysimeter ETa quantification

The first step of the validation process included the determination of ETa which was done using the water balance approaches. The objective of this step was to generate ground reference data for the extrapolation model development and validation.

Step 2. Selection of the reference evapotranspiration model

The FAO-56 Penman-Monteith model was used to calculate the reference evapotranspiration for all the stations within the irrigation scheme. The objective behind introducing ETo estimation in this study was to establish a comparative dataset to compare with ETa. This was to allow the extrapolation of ETa through ETo which is normally estimated using weather station data. This allows the estimation of ETa without using crop specific coefficients as normally done through the FAO-56 methods. The reference ET Penman–Monteith model calculates ET using the following equation:

$$ET_o = \frac{0.408\Delta(R_a - G) + \gamma\left(\frac{900}{T+273}\right)u_2(e_s - e_a)}{\Delta + \gamma(1 + 0.34u_2)} \tag{5}$$

where Δ notation represents the slope of saturated vapor pressure against the temperature curve in Kpa $^{\circ}C^{-1}$, Rn denotes the total daily net radiation in $MJm^2\ day^{-1}$, G represents the total net soil heat flux, Υ denotes the psychrometric constant in Kpa $^{\circ}C^{-1}$, T represents the average daily temperature in °C, U_2 represents the average daily wind speed in m s^{-1}, e_s represents the average daily saturated vapor pressure in Kpa, and e_a represents the average daily actual vapor pressure in Kelvin (K).

Step 3. Relationship between ETa and ETo

To develop a method to extrapolate ETa from the lysimeter point scale to multiple stations, days with unstressed water conditions were selected, this is where the first

and the second objective of the stepwise approach combine to develop an extrapolation model which was the third objective. This is because, under unstressed conditions, ETa and ETo are closer to each other, whereas under stressed conditions, ETa and ETo are far apart. To determine unstressed conditions, soil moisture data from the lysimeter was used to aid in selection where days with high moisture values $\geq$20%. This process was followed in the study of Doležal et al. (2018). A linear regression analysis was used to develop a relationship between ETa and ETo given by equation (6):

$$\mathrm{ETa} = \mathrm{a} \times \mathrm{ETo} + \mathrm{b} \tag{6}$$

where a and b are regression coefficients.

Step 4. Extrapolation model testing and validation

The developed model was tested prior use in extrapolating ETa values using station data. The performance of the model in estimating ETa was validated using statistical measures, which included r, R^2, RMSE, MAE and bias, to ensure its reliability in the extrapolation process. The dataset was split into training and validation sets at 70% and 30%, respectively. The use of 70% training ensured that there was more data across the four seasons to develop a more accurate model. The calibration of the model was based on the training set, whereas model testing was performed with the validation set to assess its predictive accuracy. The calibrated model was applied to the ETo values from all weather stations within the irrigation scheme to extrapolate ETa. The ETa values extrapolated for different weather stations in the irrigation scheme were used to validate the accuracy of the three global ET products.

Step 5. Evaluation of different global ET products at the pixel level.

The extracted ETa values from different global ET products were directly compared at their original scale with the ETa values determined from each weather station point. To match the temporal resolution averaged value for each product's pixel, the lysimeter-extrapolated values were summed to match the desired resolution. To limit errors in variables which are potentially missed by each product, meteorological variables which includes measurement of rainfall and irrigation were captured at each station making it easier reduce errors. Five statistical metrics were used to evaluate the accuracy of satellite ETa data with ground-based ETa values. These metrics include Pearson's correlation coefficient (r), bias (B), mean absolute error (MAE), and root mean square error (RMSE). Below are the mathematical expressions that define each of the used metrics:

$$\mathrm{r} = \frac{\sum_{\mathrm{i}=1}^{\mathrm{n}} (\mathrm{x_i} - \overline{\mathrm{x}})(\mathrm{y_i} - \overline{\mathrm{y}})}{\sqrt{\left(\sum_{\mathrm{i}=1}^{\mathrm{n}} (\mathrm{x_i} - \overline{\mathrm{x}})^2\right) \sum_{\mathrm{i}=1}^{\mathrm{n}} (\mathrm{y_i} - \overline{\mathrm{y}})^2)^2}} \tag{7}$$

$$\mathrm{MAE} = \frac{1}{\mathrm{n}} \sum_{\mathrm{i}=1}^{\mathrm{n}} \left|\mathrm{x_i} - \mathrm{y_i}\right| \tag{8}$$

$$\mathrm{RMSE} = \frac{1}{n}\sum_{i=1}^{n}(x_i - y_i)^2 \tag{9}$$

$$\mathrm{MAPE} = \left(\frac{1}{n}\right) \times \sum\left(\left|\frac{(\mathrm{ETa} - \ \mathrm{Estimated\ ETa})}{\mathrm{ETa}}\right|\right) \times 100 \tag{10}$$

$$\mathrm{Bias} = \overline{x} - \overline{y} \tag{11}$$

In the given equations, n denotes the sample size, xi represents the modelled ET, and yi represents the observed ET, with i indicating the sample number at the i^{th} position. Importantly, for these equations to be applied accurately, the units of xi and y^i must be the same.

3. Results

3.1. Relationship between reference evapotranspiration and actual evapotranspiration

The daily variation between actual evapotranspiration (ETa) and reference evapotranspiration (ETo) under non-stressed conditions is illustrated in Figure 5. The graph indicates a clear linear relationship between ETa and ETo when plants are not experiencing stress. There is a positive correlation between ETa and ETo, with a correlation coefficient of 0.98 and an R^2 of 0.96 (Figure 6).

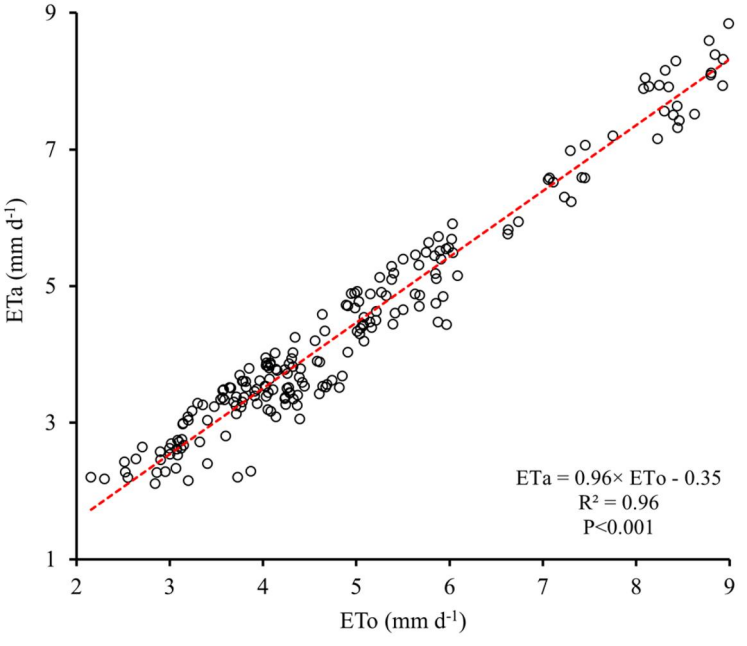

Figure 5. A daily comparison between ETa and ETo for days when the field crops were unstressed ($\theta \geq 20\%$) was used for the extrapolation of ETa using ETo at different weather stations.

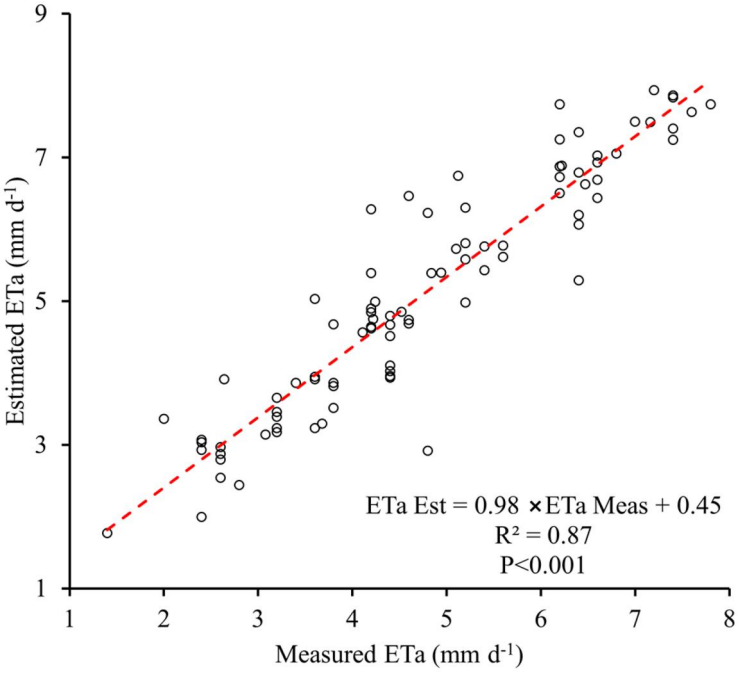

Figure 6. Daily difference between measured ETa and estimated ETa at the field scale.

3.2. Relationship between estimated ETa and field–measured ETa

This section presents a comparative analysis between ground extrapolated ETa and remotely sensed ETa estimates derived from the MOD16, WaPOR and NOAH products. The relationships are illustrated using scatter plots (Figures 7 to 10), with each plot showing linear regression lines and corresponding correlation coefficients values.

3.3. Correlation scatterplots between the station ETa and the product ETa

3.3.1. Correlation analysis of satellite ETa products at the SABBI station

Figure 7 shows the relationships between the ETa products and station ETa across the four seasons (2019, 2019–2020, 2020 and 2021) at the SABBI station. Figure 7(a) shows a negative correlation of the MOD16 pixel with the station ETa in 2019, whereas from the 2019–2020, 2020 and 2021 seasons, the correlation was positive and increased from 0.41, 0.55 to 0.68, respectively. The NOAH product demonstrated negative correlations, as indicated in Figure 7(b). A positive correlation was observed for the WaPOR product, with correlation coefficients ranging between 0.73 and 0.75.

3.3.2. Correlation analysis of satellite ETa products at the Tadcaster station

Figure 8 shows the linear relationships explored between the ETa products by the MOD16, NOAH and WaPOR products and the station ETa across the four seasons (2019, 2019–2020, 2020 and 2021) at the Tadcaster station. Figure 8(a) shows a negative correlation of the MOD16 pixel with the station ETa in the 2019 and 2019–2020 seasons, whereas from the 2020–2021 seasons, the correlation increased to 0.34 in 2020 and decreased to 0.2 in 2021. The NOAH product demonstrated negative

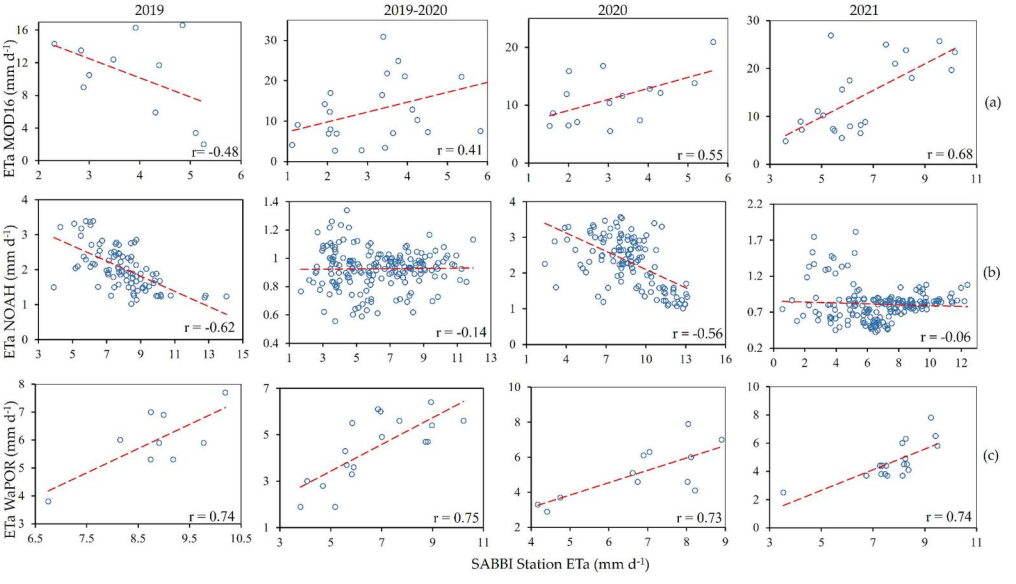

Figure 7. Correlation plots comparing MOD16 ETa, NOAH ETa, WaPOR ETa and station–derived ETa at the SABBI station.

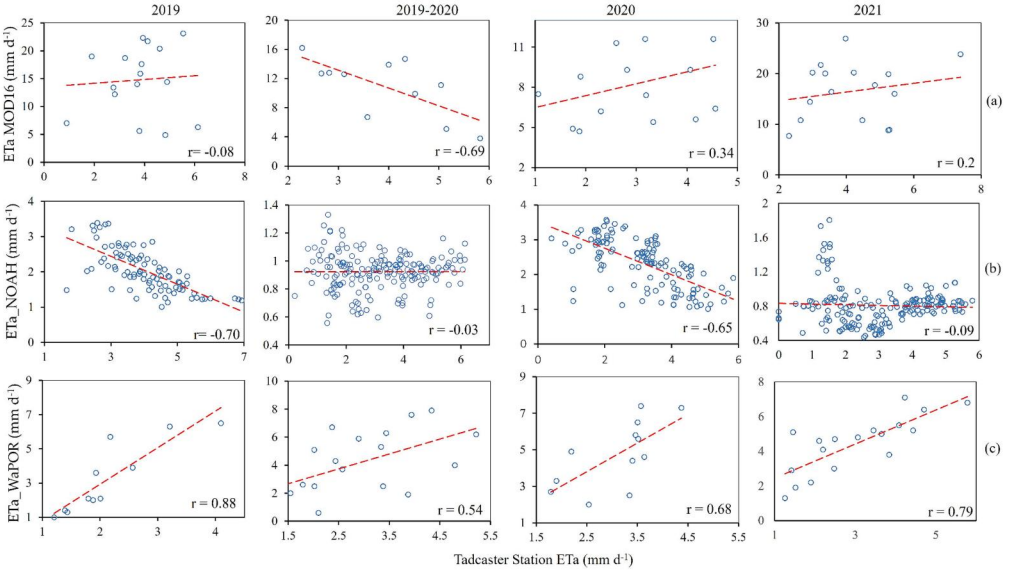

Figure 8. Correlation plots comparing MOD16 ETa, NOAH ETa, WaPOR ETa and station–derived ETa at the Tadcaster station.

correlations. A positive correlation was observed for the WaPOR product, with correlation coefficients ranging between 0.54 and 0.81 across the four seasons.

3.3.3. Correlation analysis of satellite ETa products at the Ganspan station

Figure 9 shows a linear relationship between the ETa products of the MOD16, NOAH and WaPOR products and the station ETa across the four seasons (2019, 2019–2020,

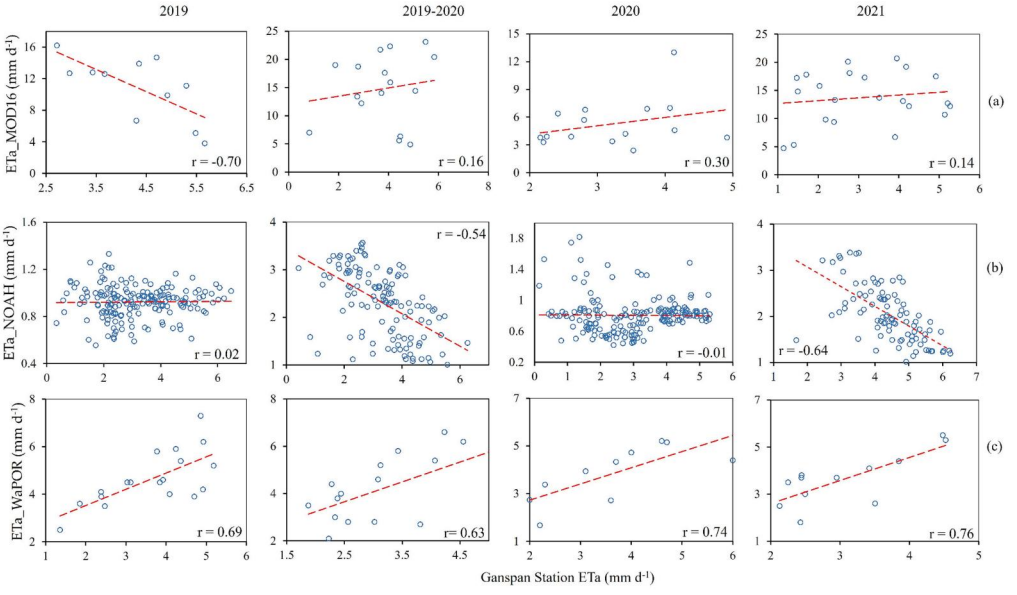

Figure 9. Correlation plots comparing all evaluated products at Ganspan station.

2020 and 2021) at the Ganspan station. Figure 9(a) shows a negative correlation between MOD16 pixels and station ETa in the 2019 season, whereas from the 2019–2020 seasons to the 2021 season, the correlation was slightly positive, indicating a poor correlation. The NOAH product demonstrated negative correlations, as indicated in Figure 9(b), although some good negative correlations of −0.54 and −0.64 were obtained during the 2019–2020 and 2021 seasons, which, however, do not explain field ETa accurately. A positive correlation was observed for the WaPOR product, with correlation coefficients ranging between 0.55 and 0.76 across the four seasons.

3.3.4. Correlation analysis of satellite ETa products at Jankempdorp station

Figure 10 shows the linear relationships explored between the ETa products by MOD16, NOAH and WaPOR products and the station ETa across the four seasons (2019, 2019–2020, 2020 and 2021) at Jankempdorp station. MOD16 shows negative correlation as well as the NOAH pixel across most seasons. The WaPOR pixel demonstrated good correlations except in 2020.

3.4. Evaluation of the ETa products at the SABBI meteorological station across seasons

3.4.1. Evaluation of MOD16 at the SABBI station

The evaluation statistics across different time periods, i.e. the 2019 winter, 2019–2020 summer, 2020 winter and 2021 summer seasons, were obtained using comparative analyses between MOD16 pixels and extrapolated ETa at the SABBI meteorological station (Table 3). The statistical metrics of each season indicate that the MOD16 model's performance improved over time from 2019 to 2021. Although the 2021 season was the only season with significant correlations.

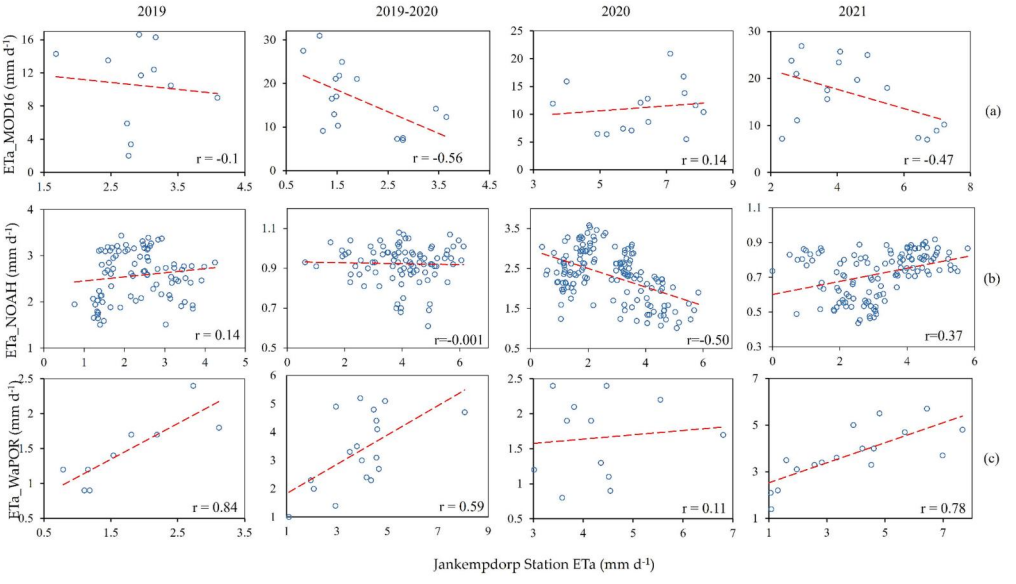

Figure 10. Correlation plots comparing MOD16 ETa, NOAH ETa, WaPOR ETa and station–derived ETa at the Jankempdorp station.

Table 3. Statistical metrics of the evaluation between MOD16 and station ETa at SABBI.

	SABBI Station MOD16						
SABBI MOD16	R	R^2	RMSE	MAE	BIAS	MAPE	*p* value
2019	−0.48	0.23	8.48	7.56	−6.66	74.87	$p > 0.05$
2019–2020	0.41	0.16	12.3	9.63	−9.62	63.38	$p > 0.05$
2020	0.55	0.3	3.58	2.79	-2.37×10^{-16}	28.65	$p > 0.05$
2021	0.68	0.47	5.45	4.26	2.06×10^{-15}	37.81	$p < 0.001$

Table 4. Statistical metrics of the evaluation between NOAH and station ETa at SABBI.

	SABBI Station NOAH						
SABBI NOAH	R	R^2	RMSE	MAE	BIAS	MAPE	*p* value
2019	−0.62	0.39	0.47	0.38	-2.44×10^{-16}	20.30	$p < 0.001$
2019–2020	−0.14	0.02	0.15	0.11	-3.49×10^{-16}	12.94	$p > 0.05$
2020	−0.56	0.32	7.02	6.45	6.45	35.01	$p < 0.001$
2021	−0.06	0.004	6.51	6.02	6.02	80.13	$p > 0.05$

3.4.2. Evaluation of NOAH at the SABBI station

The evaluation of NOAH pixels at the SABBI meteorological station is presented with statistical metrics in Table 4. The table compares ETa estimated data from the SABBI station with the NOAH ETa product pixel over different seasonal periods from the 2019 winter season, 2019–2020 summer, 2020 winter season and 2021 summer seasons, demonstrating the product's performance with different statistical metrics. In the 2019 season, the NOAH product demonstrated a negative correlation value, with an r value of −0.62 and a low R^2 value of 0.39, a relatively low RMSE of 0.47 and a MAPE of 20.3%. Poor negative correlations and high errors were obtained across other seasons.

Table 5. Evaluation statistical metrics between WaPOR and the station ETa at SABBI.

SABBI Station WaPOR							
SABBI WaPOR	R	R^2	RMSE	MAE	BIAS	MAPE	*p* value
2019	0.74	0.55	2.95	2.85	−2.85	32.56	$p < 0.05$
2019–2020	0.75	0.56	2.58	2.29	−2.29	34.08	$p < 0.001$
2020	0.73	0.54	2.02	1.7	−1.7	24.68	$p < 0.001$
2021	0.74	0.55	3.22	3.09	3.09	39.75	$p < 0.001$

Table 6. Statistical metrics of the evaluation between MOD16 and station ETa at Tadcaster.

Tadcaster MOD16							
Tadcaster MOD16	R	R^2	RMSE	MAE	BIAS	MAPE	*p* value
2019	−0.08	0.01	12.52	10.97	−10.97	65.8	$p > 0.05$
2019–2020	−0.69	0.48	8.36	7.30	−6.92	81.38	$p < 0.05$
2020	0.34	0.11	5.89	5.26	−5.26	70.07	$p > 0.05$
2021	0.20	0.04	13.49	12.32	−12.31	71.40	$p > 0.05$

Table 7. Statistical metrics of the evaluation between NOAH and station ETa at Tadcaster.

Tadcaster NOAH							
Tadcaster NOAH	R	R^2	RMSE	MAE	BIAS	MAPE	*p* value
2019	−0.7	0.49	2.52	2.12	1.99	1.32	$p < 0.001$
2019–2020	−0.03	0.01	0.13	0.10	0.01	11.56	$p > 0.05$
2020	−0.65	0.43	1.95	1.63	0.87	0.93	$p < 0.001$
2021	−0.09	0.01	2.71	2.33	2.31	31.95	$p > 0.05$

3.4.3. Evaluation of WaPOR at the SABBI station

The WaPOR ETa product was evaluated at the SABBI station, resulting in the statistical metrics presented in Table 5. The table compares the ETa data from the SABBI station with those from the WaPOR pixel for the periods 2019, 2019–2020, 2020 and 2021. Fairly good correlations were achieved across all seasons supported by highly statistically significant p-values ($p < 0.001$).

3.5. Evaluation of ETa products at the Tadcaster meteorological station across seasons

3.5.1. Evaluation of MOD16 at Tadcaster station

Table 6 shows the performance of the MOD16 ETa product pixel at the Tadcaster meteorological station over different periods, which shows varying results.

3.5.2. Evaluation of NOAH at the Tadcaster station

A comparison between the NOAH product and station ETa at the Tadcaster station is presented in Table 7. The comparison of NOAH ETa with station ETa for different periods from 2019–2020 and 2020–2021 reveals poor agreement. For example, during the winter 2019 season, the NOAH ETa product shows a strong negative correlation with an r value of −0.7 and a moderate R^2 value of 0.49, with an RMSE of 2.52 mm d^{-1}, an MAE value of 2.12 mm d^{-1}, and a negative bias value of 1.99, which suggests consistent underestimation of ETa. Negative correlations were obtained across all seasons.

Table 8. Statistical metrics of the evaluation between the WaPOR and station ETa at Tadcaster.

Tadcaster WaPOR							
Tadcaster WaPOR	R	R^2	RMSE	MAE	BIAS	MAPE	*p* value
2019	0.88	0.78	1.72	1.17	−1.11	25.89	$p < 0.001$
2019–2020	0.54	0.29	2.23	1.86	−1.27	52.38	$p < 0.05$
2020	0.68	0.46	2.14	1.88	−1.65	37.62	$p < 0.05$
2021	0.79	0.63	1.72	1.42	−1.42	30.29	$p < 0.001$

Table 9. Statistical metrics of the evaluation between MOD16 and station ETa at Ganspan.

Ganspan MOD16							
Ganspan MOD 16	R	R^2	RMSE	MAE	BIAS	MAPE	*p* value
2019	−0.70	0.49	7.99	6.95	−6.55	57.78	$p < 0.05$
2019–2020	0.16	0.02	12.48	10.99	−10.99	67.05	$p > 0.05$
2020	0.30	0.08	3.15	2.34	−2.05	39.32	$p > 0.05$
2021	0.14	0.02	11.52	10.59	−10.59	74.74	$p > 0.05$

3.5.3. Evaluation of WaPOR at the Tadcaster station

Table 8 compares the ETa data obtained from the Tadcaster station with those of the WaPOR product for different periods from 2019 winter, 2019–2020 summer, 2020 winter and 2021 summer. The results demonstrate the good performance of the WaPOR product in estimating ETa. In the 2019 winter season, the WaPOR product shows a strong positive correlation with an r value of 0.88 and a high R^2 value of 0.78, with relatively low error values shown by an RMSE value of 1.72 mm d^{-1} and an MAE of 1.17 mm d^{-1}, although the negative bias value of −1.11 indicates a slight underestimation by the WaPOR product.

3.6. Evaluation of ETa products at the Ganspan meteorological station across seasons

3.6.1. Evaluation of MOD16 at the Ganspan station

Table 9 shows a comparison of the ETa data from the Ganspan station and the MOD16 product over several periods, including the 2019 winter, 2019–2020 summer, 2020 winter and 2021 summer seasons, reflecting weak to moderate agreement. In the 2019 season, the MOD16 product shows a negative correlation, with an r value of −0.70 and an R^2 value of 0.49. However, the error metrics demonstrated by the RMSE value of 7.99 mm d^{-1}, the MAE of 6.95 mm d^{-1} and a negative bias of −6.55 show that the product consistently underestimated ETa, with a higher MAPE of 57.78%.

3.6.2. Evaluation of NOAH at the Ganspan station

Table 10 compares the ETa estimates from the Ganspan station with those from the NOAH product pixel for different periods ranging from 2019–2020 and 2020–2021, demonstrating the poor performance of the NOAH product. During the 2019 season, the correlation appears to be non–existent, with an r value of 0.02 and a very low R^2 value of 0.0003, indicating that the model has no predictive power. The error metric yields an RMSE value of 2.62 mm d^{-1}, with an MAE value of 2.28 mm d^{-1}, which is

Table 10. Statistical metrics of the evaluation between NOAH and station ETa at Ganspan.

	Ganspan ETa NOAH						
Ganspan NOAH	r	R^2	RMSE	MAE	BIAS	MAPE	*p* value
2019	0.02	0.0003	2.62	2.28	2.26	25.78	$p > 0.05$
2019–2020	−0.54	0.29	1.90	1.56	1.01	89.49	$p < 0.001$
2020	−0.01	0.0002	2.56	2.24	2.19	97.75	$p > 0.05$
2021	−0.64	0.41	2.75	2.43	2.39	47.62	$p < 0.001$

Table 11. Statistical metrics of the evaluation between the WaPOR and station ETa at Ganspan.

	Ganspan WaPOR						
Ganspan WaPOR	r	R^2	RMSE	MAE	BIAS	MAPE	*p* value
2019	0.69	0.48	1.34	1.19	−1.01	26.28	$p < 0.001$
2019–2020	0.63	0.39	1.48	1.3	−1.03	28.84	$p < 0.001$
2020	0.74	0.55	0.87	0.81	0.21	24.41	$p < 0.001$
2021	0.76	0.58	0.89	0.84	−0.58	24.10	$p < 0.001$

Table 12. Statistical metrics of evaluation between MOD16 and station ETa at Jankempdorp.

	Jankempdorp MOD 16						
Jankempdorp MOD16	r	R^2	RMSE	MAE	BIAS	MAPE	*p* value
2019	−0.1	0.01	8.99	7.73	−7.59	64.93	$p > 0.05$
2019–2020	−0.56	0.32	16.38	14.40	−14.4	83.73	$p < 0.05$
2020	0.14	0.02	6.52	5.18	−4.9	40.61	$p > 0.05$
2021	−0.47	0.22	14.63	12.32	−12.32	64.0	$p > 0.05$

relatively high. The positive bias value of 2.26 shows that the product overestimates ETa.

3.6.3. Evaluation of WaPOR at the Ganspan station

The results in Table 11 compare ETa data from the Ganspan meteorological station with the WaPOR ETa product across 2019, 2019–2020, 2020 and 2021. During the 2019 cropping season, the WaPOR ETa product shows a strong positive correlation with an r value of 0.69 and an R^2 value of 0.48, while it shows moderate errors, with an RMSE value of 1.34 mm d^{-1}, an MAE value of 1.19 mm d^{-1} and a slight underestimation, as shown by the bias value of −1.01. The product's accuracy is supported by a highly statistically significant p value < 0.001.

3.7. Evaluation of ETa products at the Jankempdorp meteorological station across seasons

3.7.1. Evaluation of MOD16 at Jankempdorp station

The statistical metrics shown in Table 12 compare the ETa data from the Jankempdorp meteorological station with those from the MOD16 product across the 2019, 2019–2020, 2020 and 2021 seasons. The results demonstrate that, in 2019, the products show a very weak correlation with station ETa, as indicated by an r value of −0.1 and a low R^2 value of 0.01, with high error values indicated by an RMSE value of 8.99 mm d^{-1}, an MAE value of 7.73 mm d^{-1} and significant underestimation, as indicated by a bias value of −7.59. The high MAPE of 64.93% and a non–

Table 13. Statistical metrics of the evaluation between NOAH and station ETa at Jankempdorp.

Jankempdorp NOAH							
Jankempdorp NOAH	r	R^2	RMSE	MAE	BIAS	MAPE	*p* value
2019	0.14	0.02	0.96	0.81	−0.23	32.41	$p > 0.05$
2019–2020	−0.03	0.01	3.28	3.07	−3.06	67.56%	$p > 0.05$
2020	−0.50	0.25	1.78	1.48	−0.43	65.38	$p < 0.001$
2021	0.37	0.14	0.12	0.10	6.58×10^{-16}	15.22	$p < 0.001$

Table 14. Statistical metrics of the evaluation between WaPOR and station ETa at Jankempdorp.

Jankempdorp WaPOR							
Jankempdorp WaPOR	r	R^2	RMSE	MAE	BIAS	MAPE	*p* value
2019	0.84	0.71	0.52	0.37	0.27	24.88	$p < 0.05$
2019–2020	0.59	0.34	1.38	1.03	0.58	35.07	$p < 0.05$
2020	0.11	0.01	2.87	2.66	2.66	93.55	$p > 0.05$
2021	0.80	0.61	1.38	1.12	−0.02	32.58	$p < 0.001$

significant p–value of >0.05 demonstrate the poor performance of the MOD16 product. During the 2019–2020 season, the correlation improved to a coefficient value of −0.56, with an R^2 value of 0.32, which indicates some predictive power. However, the error metrics are very high, with an RMSE value of 16.38 mm d^{-1} and an MAE value of 14.4 mm d^{-1}, whereas a very large negative bias value of −14.4 shows a substantial underestimation of ETa by the product.

3.7.2. Evaluation of NOAH at Jankempdorp station

The statistical metrics shown in Table 13 demonstrate that, in 2019, the NOAH ETa products had a very weak correlation with the Jankempdorp meteorological station ETa, with an r value of 0.14 and an R^2 value of 0.02, which indicates very low predictive power. However, the RMSE value is low, with a value of 0.96 mm d^{-1} and a low MAE value of 0.81 mm d^{-1}, with a small negative bias value of −0.23 and a MAPE value of 32.41%. The p value is >0.05, which suggests that the product's performance is not statistically significant. For 2019–2020, the product shows a nearly negligible correlation, with an r value of −0.03 and an R^2 value of almost zero at 0.0009. The results demonstrate higher error metrics, with an RMSE value of 3.28 mm d^{-1}, an MAE value of 3.07 mm d^{-1} and a large bias value of −3.06, which indicates an underestimation of ETa. The p value >0.05 indicates that there is no statistical significance.

3.7.3. Evaluation of WaPOR at the Jankempdorp station

During the 2019 season, the statistical metrics shown in Table 14 highlight the relationships between the WaPOR ETa pixel and the Jankempdorp weather station ETa values. The WaPOR product has a strong positive correlation coefficient value of 0.84, with a high R^2 value of 0.71, which indicates good predictive performance. The errors appear to be low, with an RMSE value of 0.52 mm d^{-1}, an MAE value of 0.37 mm d^{-1} and a low positive bias value of 0.27. In 2020 high errors and low correlations were achieved with insignificant p value. Significant correlations were achieved in 2019-2020 and 2021 seasons.

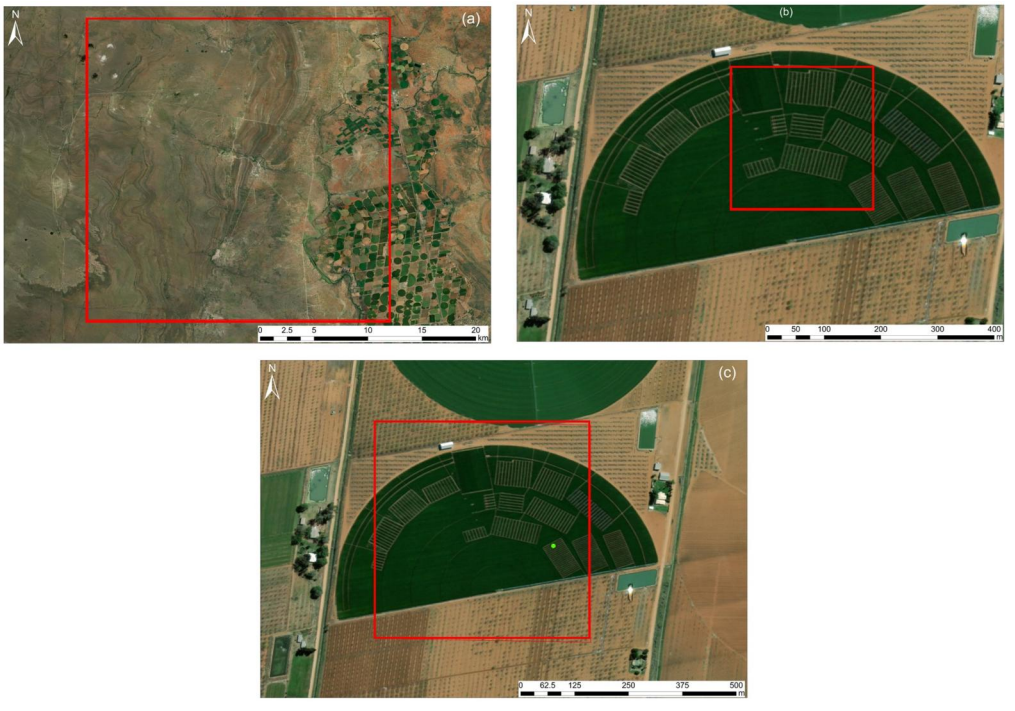

Figure 11. The NOAH (a), WaPOR (b) and MOD16 (c) pixels with reference to the experimental farm.

3.8. Products spatial coverage with reference to the experimental farm and the surrounding areas

Figure 11(a–c) depicts the location of the experimental farm's lysimeter setting point and a single pixel coverage. Figure 11(a) shows the NOAH pixel which appears to cover multiple farms and non-agricultural landscapes. Figure 11(b) shows the WaPOR pixel which appears to capture the experimental farm cropped area fully, while Figure 11(c) shows the MOD16 pixel covering the experimental farm and extending beyond the farm boundaries to the neighbouring farms.

4. Discussion

This study aimed to evaluate the accuracy of MOD16, NOAH and WaPOR ETa products within the Vaalharts irrigation scheme using a multi-step approach in which farm-scale measurements were extrapolated to different locations with meteorological stations. This was influenced by the limitation of direct ETa measurements being the biggest data gap in South Africa's agricultural water management. It was also necessary to evaluate these products because they were developed and validated in areas outside South African agricultural regions. The findings of this study demonstrated that MOD16 and NOAH ETa products are still far from being representative of ETa at farm scales, whereas WaPOR ETa showed promising correlations in most instances.

The evaluation results demonstrated that MOD16 performs poorly in estimating crop water use or ETa in irrigated agricultural landscapes of South Africa. Ramoelo et al. (2014) reported the poor performance of MOD16 in South African semi-arid regions when compared with eddy covariance measurements in non-agricultural environments. Several studies have also reported similar findings to our findings which they attributed their errors to spatial mismatch and energy balance closure issues on eddy covariance systems (Ramoelo et al. 2014; Jovanovic et al. 2015; Majozi et al. 2017; Ndara 2017). This study evaluated MOD16 at a 500 m spatial resolution in agricultural areas with diverse crops and irrigation practices, while Ramoelo et al. (2014) focused on MOD16 at a 1 km resolution in savanna and woodland ecosystems. Although validation approaches differ, this study found similar spatial and seasonal estimation errors. The underestimation of ETa by MOD16, as demonstrated through negative bias values, agree with results reported in the Central Plains of the United States (Velpuri et al. 2013) and arid environments of Europe (Hu et al. 2015). However, MOD16 has been proven to perform well in humid environments, as demonstrated by Mu et al. (2011) and Liu et al. (2013) in China. Dzikiti et al. (2019) attempted to improve MOD16 accuracy in the Western Cape by adjusting input parameters, yielding better performance, this demonstrates the challenges of MOD16 product algorithm parameterization. The validation approach used in this study was aimed to quantify ETa in non-stressed conditions, however, it is possible that when irrigation inputs differed in one pixel, it affected the moisture levels being inaccurately averaged. The averaged moisture affects ETa estimation which is accurately captured on ground resulting in poor satellite estimated ETa. The inability of MOD16 to capture soil moisture variability when the product pixel covers multiple farms with different irrigation practices is supported by Souza et al. (2019), who found poor correlations with eddy covariance data in Brazilian rice farms. This makes MOD16 less suitable for agricultural water management.

The inaccuracies of the NOAH ET product could be associated with the spatial resolution of the GLDAS data, which is 0.25°. This coarse resolution is inadequate for capturing local variations in heterogeneous agricultural landscapes. While NOAH has a temporal resolution of three hours which allows synchronization with high-temporal-resolution data, its performance varies significantly across weather stations. This demonstrates its variability in geographical regions, for example, NOAH performs well in humid eastern China but poorly in arid western China due to soil moisture deficits (Qi et al. 2015; Yin et al. 2023). Li et al. (2024) found that NOAH estimates crop water footprints well in humid areas but poorly in arid and semi-arid environments. Similarly, Ma et al. (2017) reported a 22% overestimation of ET in the United States due to inaccuracies in the vegetation model within the GLDAS algorithm. This study also found that NOAH overestimated ETa across multiple seasons, indicating that it does not fully capture vegetation and land surface variations.

Among the three evaluated products, WaPOR demonstrated moderate to high correlations with in-situ measurements, with correlation coefficients reaching 0.88. These findings are supported by the findings of Blatchford et al. (2020) who assessed WaPOR in Africa against eddy covariance systems and found good correlations in South Africa's Kruger National Park, though they acknowledged inherent eddy

covariance errors (~30%). Their findings demonstrate the capabilities of WaPOR to accurately estimate ETa in South African environments. This study, however, focused on irrigated agriculture, integrating weighing lysimeter data with weather station records. The lower correlations observed here compared to Chukalla et al. (2022) in Mozambique who reported the highest R^2 of 0.91 could be attributed to differences in spatial resolution of 250 m used in this study versus their used resolution of 100 m. Despite its advantages, WaPOR's accuracy depends on input data quality and resolution. The MODIS land cover layer, used in WaPOR (1 km resolution), introduces errors by averaging diverse land covers within a pixel. Kaan (2024) evaluated WaPOR v3 in Belgium, Germany, and France, obtaining correlation coefficients between 0.72 and 0.82, these values are comparable to this study findings. Moreover, Geshnigani et al. (2021) found strong agreement between WaPOR-derived ET and estimates from the Penman-Monteith and Modified Hargreaves and Samani models derived crop ET. Unlike these approaches, this study provides ETa directly, eliminating the need for crop coefficients.

The good performance obtained in this study can be attributed to WaPOR pixels being representative of the field conditions while it is able to represent an individual farm without boundary sharing effects. Findings of this study confirms the findings made by Fakhar & Kaviani (2014) who obtained high correlations of WaPOR and measured ETa in Iran. This suggest that WaPOR can capture the soil, plant-water dynamics of an individual farm. Further analysis on the performance of WaPOR across different regions comparing similar product evaluations highlight regional differences in ETa estimation accuracy. For example, Garatuza-Payan et al. (2022) found that WaPOR underestimated ETa in semi-arid environments of Mexico. Similarly, the underestimations by WaPOR on this study could be attributed to moisture deficit. These findings demonstrate the importance of site-specific assessments, this is because generalizing model performance across different regions can be misleading. Furthermore, the integration of remote sensing ETa with soil moisture indices has proven to be beneficial in addressing some of the limitations as demonstrated by Sejine and Anane (2025) where soil moisture data improved WaPOR's accuracy in estimating ETa. In the current study we found that integrating lysimeter water balance data helped in the evaluation of WaPOR product, this is because the lysimeter uses changes in moisture which relates to the findings by Sejine and Anane (2025) on soil moisture integration.

The uncertainties associated with remote sensing ETa products emerge from the algorithms which are used to generate them (Mu et al. 2011; Ramoelo et al. 2014). Coarse resolution products introduce high errors due to inaccurate land cover classification particularly in heterogeneous environments like the Vaalharts irrigation scheme where pixels include irrigation dams, pecan trees, and roads. This variability affects soil moisture values and land surface temperatures (LSTs), introducing errors in ET estimation. In addition, remote sensing models estimate ET instantaneously at satellite overpass times, making temporal integration challenging. Differences in irrigation schedules among adjacent farms further complicate moisture variability estimation affecting aerodynamic terms in ET models (Ratshiedana et al. 2025). The limited availability of ground-based observations constrains ETa validation, leading to uncertainties in regional water balance assessments.

This study bridges the gap between in-situ and satellite-derived ETa estimates by incorporating high-precision lysimeter measurements, providing a refinement in the accuracy and reliability of remote sensing ETa products. The site-specific ETa measurements enabled precise evaluation of biases and uncertainties, demonstrating the necessity of hybrid approaches that integrate in-situ and satellite data for improved agricultural water management. The inclusion of lysimeter data provides a crucial benchmark, ensuring that future refinements in remote sensing ETa products consider regional variability, irrigation practices and land use heterogeneity.

5. Conclusions

This study evaluated the accuracy of MOD16, NOAH and WaPOR global remote sensing ETa products under different seasons in the Vaalharts irrigation scheme. The findings of this study confirm that WaPOR is a valuable tool for quantifying crop water use. Contrary, results demonstrated that MOD16 and NOAH products exhibited poor accuracies due to their coarse resolutions. This study demonstrated a stepwise validation approach which allows generation of ETa in the absence of direct measurement tools offering a practical solution for areas with limited measurement infrastructure. There is a need for improved parameterization in MOD16 and NOAH products to enhance their applicability in agricultural environments. Future research should focus on refining ETa estimation algorithms integrating higher-resolution datasets and expanding the availability of WaPOR's 30 m resolution for more detailed agricultural water assessments.

Acknowledgement

We would like to acknowledge the South African Barley Breeding Institute for providing their experimental farm for this study and the Arid Region Water Research Centre, Sol Plaatje University for their support.

Author contributions

PER: conceptualization, data curation, formal analysis, investigation, methodology, software, validation, visualization, and writing original draft preparation. MAM, EA, GC: conceptualization, funding acquisition, investigation, project administration, supervision and validation.

Disclosure statement

No potential conflict of interest was reported by the author(s).

Funding

This study was funded by the Water Research Commission (WRC) of South Africa under the project: C2022_2023 – 00978, the National Research Foundation of South Africa (NRF) Grant Number: CPRR 23030681033 and the Agricultural Research Council (ARC) of South Africa under the crop estimate project: ISC012403000027.

Data availability statement

Data used and generated for this study are included in the article through links while some data is available on request.

References

Abbasi N, Nouri H, Nagler P, Didan K, Chavoshi Borujeni S, Barreto-Muñoz A, Opp C, Siebert S. 2023. Crop water use dynamics over arid and semi-arid croplands in the lower Colorado River Basin. Eur J Remote Sens. 56(1):2259244. doi: 10.1080/22797254.2023.2259244.

Allen RG, Pereira LS, Raes D, Smith M. 1998. Crop evapotranspiration-Guidelines for computing crop water requirements-FAO Irrigation and drainage paper 56. Vol. 300. Rome: FAO. p. D05109.

Bashir RN, Khan FA, Khan AA, Tausif M, Abbas MZ, Shahid MMA, Khan N. 2023. Intelligent optimization of Reference Evapotranspiration (ETo) for precision irrigation. J Comput Sci. 69:102025. doi: 10.1016/j.jocs.2023.102025.

Bashir RN, Mzoughi O, Shahid MA, Alturki N, Saidani O. 2024. Principal Component Analysis (PCA) and feature importance-based dimension reduction for Reference Evapotranspiration (ET0) predictions of Taif, Saudi Arabia. Comput Electron Agric. 222: 109036. doi: 10.1016/j.compag.2024.109036.

Blatchford ML, Mannaerts CM, Njuki SM, Nouri H, Zeng Y, Pelgrum H, Wonink S, Karimi P. 2020. Evaluation of WaPOR V2 evapotranspiration products across Africa. Hydrol Process. 34(15):3200–3221. doi: 10.1002/hyp.13791.

Bodner G, Nakhforoosh A, Kaul HP. 2015. Management of crop water under drought: a review. Agron Sustain Dev. 35(2):401–442. doi: 10.1007/s13593-015-0283-4.

Chukalla AD, Mul ML, Van Der Zaag P, Van Halsema G, Mubaya E, Muchanga E, Den Besten N, Karimi P. 2022. A framework for irrigation performance assessment using WaPOR data: the case of a sugarcane estate in Mozambique. Hydrol Earth Syst Sci. 26(10): 2759–2778. doi: 10.5194/hess-26-2759-2022.

Djaman K, O'Neill M, Owen C, Smeal D, Koudahe K, West M, Allen S, Lombard K, Irmak S. 2018. Crop evapotranspiration, irrigation water requirement and water productivity of maize from meteorological data under semiarid climate. Water. 10(4):405. doi: 10.3390/w10040405.

Doležal F, Hernandez-Gomis R, Matula S, Gulamov M, Miháliková M, Khodjaev S. 2018. Actual evapotranspiration of unirrigated grass in a smart field lysimeter. Vadose Zone J. 17(1):1–13. doi: 10.2136/vzj2017.09.0173.

Du Plessis A, editor. 2019. Evaluation of Southern and South Africa's freshwater resources. Cham, Switzerland: Springer Water. p. 147–172. doi: 10.1007/978-3-030-03186-2_7.

DWS. 2006. DWS Home. Pretoria, South Africa: DWS. [accessed 2024 October 30]. https://www.dws.gov.za/WAR/documents/VerificationGuide2EdNov06.pdf.

Dzikiti S, Jovanovic NZ, Bugan RD, Ramoelo A, Majozi NP, Nickless A, Cho MA, Le Maitre DC, Ntshidi Z, Pienaar HH. 2019. Comparison of two remote sensing models for estimating evapotranspiration: algorithm evaluation and application in seasonally arid ecosystems in South Africa. J Arid Land. 11(4):495–512. doi: 10.1007/s40333-019-0098-2.

Elfarkh J, Simonneaux V, Jarlan L, Ezzahar J, Boulet G, Chakir A, Er-Raki S. 2022. Evapotranspiration estimates in a traditional irrigated area in semi-arid Mediterranean. Comparison of four remote sensing-based models. Agric Water Manage. 270:107728. doi: 10.1016/j.agwat.2022.107728.

Fakhar MS, Kaviani A. 2024. Estimation of water consumption volume and water efficiency in irrigated and rainfed agriculture based on the WaPOR database in Iran. J Water Clim Change. 15(6):2731–2752. doi: 10.2166/wcc.2024.655.

FAO. 2019. WaPOR quality assessment: technical report on the data quality of the WaPOR FAO database version 1.0. Rome, Italy: Food & Agriculture Organization.

Gabr ME, Awad A, Farres HN. 2024. Irrigation water management in a water-scarce environment in the context of climate change. Water Air Soil Pollut. 235(2):127. doi: 10.1007/s11270-024-06934-8.

Gabr ME. 2022. Modelling net irrigation water requirements using FAO-CROPWAT 8.0 and CLIMWAT 2.0: a case study of Tina Plain and East South ElKantara regions, North Sinai, Egypt. Arch Agron Soil Sci. 68(10):1322–1337. doi: 10.1080/03650340.2021.1892650.

Geshnigani FS, Mirabbasi R, Golabi MR. 2021. Evaluation of FAO's WaPOR product in estimating the reference evapotranspiration for stream flow modelling. Theor Appl Climatol. 144(1-2):191–201. doi: 10.1007/s00704-021-03534-y.

Gibson L, Jarmain C, Su Z, Eckardt F. 2013. Review: estimating evapotranspiration using remote sensing and the Surface Energy Balance System – a South African perspective. WSA. 39(4):477–486. doi: 10.4314/wsa.v39i4.5.

Gleick P. 2023. The most important issue about water is not supply, but how it is used. Nature. 623(7985):25. doi: 10.1038/d41586-023-03899-2.

Gutry-Korycka M. 2019. The influence of hydro-climatological balances and Nature-based solutions (NBS) in the management of water resources. Meteorol Hydrol Water Manage. 7(2):55–63. doi: 10.26491/mhwm/110415.

Hu G, Jia L, Menenti M. 2015. Comparison of MOD16 and LSA-SAF MSG evapotranspiration products over Europe for 2011. Remote Sens Environ. 156:510–526. doi: 10.1016/j.rse.2014.10.017.

Ingrao C, Strippoli R, Lagioia G, Huisingh D. 2023. Water scarcity in agriculture: an overview of causes, impacts and approaches for reducing the risks. Heliyon. 9(8):e18507. doi: 10.1016/j.heliyon.2023.e18507.

Jovanovic N, Mu Q, Bugan R, Zhao M. 2015. Dynamics of MODIS evapotranspiration in South Africa. WSA. 41(1):79. doi: 10.4314/wsa.v41i1.11.

Kaan E.R. 2024. Evaluation of the WaPOR v3 dataset for crop water productivity and precision agriculture applications [Master's thesis]. University of Twente. [accessed 2025 February 28]. https://purl.utwente.nl/essays/101168.

Khan MS, Baik J, Choi M. 2020. Inter-comparison of evapotranspiration datasets over heterogeneous landscapes across Australia. Adv Space Res. 66(3):533–545. doi: 10.1016/j.asr.2020.04.037.

Khanal S, Kc K, Fulton JP, Shearer S, Ozkan E. 2020. Remote sensing in agriculture—accomplishments, limitations, and opportunities. Remote Sens. 12(22):3783. doi: 10.3390/rs12223783.

Li P, Jia L, Lu J, Jiang M, Zheng C. 2024. A new evapotranspiration-based drought index for flash drought identification and monitoring. Remote Sens. 16(5):780. doi: 10.3390/rs16050780.

Liu SM, Xu ZW, Zhu ZL, Jia ZZ, Zhu MJ. 2013. Measurements of evapotranspiration from eddy-covariance systems and large aperture scintillometers in the Hai River Basin, China. J Hydrol. 487:24–38. doi: 10.1016/j.jhydrol.2013.02.025.

Ma N, Niu GY, Xia Y, Cai X, Zhang Y, Ma Y, Fang Y. 2017. A systematic evaluation of Noah-MP in simulating land-atmosphere energy, water, and carbon exchanges over the continental United States. JGR Atmospheres. 122(22):12–245. doi: 10.1002/2017JD027597.

Maisela RJ. 2007. Realizing agricultural potential in land reform: The case of Vaalharts irrigation scheme in the Northern Cape Province University of the Western Cape. [Thesis]. [accessed 2024 February 24]. https://etd.uwc.ac.za:443/xmlui/handle/11394/2280.

Majozi NP, Mannaerts CM, Ramoelo A, Mathieu R, Mudau AE, Verhoef W. 2017. An intercomparison of satellite-based daily evapotranspiration estimates under different eco-climatic regions in South Africa. Remote Sens. 9(4):307. doi: 10.3390/rs9040307.

Moeletsi ME, Myeni L, Kaempffer LC, Vermaak D, de Nysschen G, Henningse C, Nel I, Rowswell D. 2022. Climate dataset for South Africa by the agricultural research council. Data. 7(8):117. doi: 10.3390/data7080117.

Mu Q, Zhao M, Running SW. 2011. Improvements to a MODIS global terrestrial evapotranspiration algorithm. Remote Sens Environ. 115(8):1781–1800. doi: 10.1016/j.rse.2011.02.019.

Ndara N. 2017. Analysis of monthly MOD16 evapotranspiration rates at sites with different climatic characteristics; Heuningnes and Letaba catchments in South Africa. [Accessed 2024 September 17]. https://etd.uwc.ac.za/handle/11394/5867.

Peters A, Nehls T, Schonsky H, Wessolek G. 2014. Separating precipitation and evapotranspiration from noise – a new filter routine for high-resolution lysimeter data. Hydrol Earth Syst Sci. 18(3):1189–1198. doi: 10.5194/hess-18-1189-2014.

Qi W, Zhang C, Fu G, Zhou H. 2015. Global Land Data Assimilation System data assessment using a distributed biosphere hydrological model. J Hydrol. 528:652–667. doi: 10.1016/j.jhydrol.2015.07.011.

Ramoelo A, Majozi NP, Mathieu R, Jovanovic N, Nickless A, Dzikiti S. 2014. Validation of global evapotranspiration product (MOD16) using flux tower data in the African Savanna, South Africa. Remote Sens. 6(8):7406–7423. doi: 10.3390/rs6087406.

Ratshiedana PE, Abd Elbasit MA, Adam E, Chirima JG, Liu G, Economon EB. 2023. Determination of soil electrical conductivity and moisture on different soil layers using electromagnetic techniques in irrigated arid environments in South Africa. Water. 15(10):1911. doi: 10.3390/w15101911.

Ratshiedana PE, Abd Elbasit MA, Adam E, Chirima JG. 2025. Evaluation of micrometeorological models for estimating crop evapotranspiration using a smart field weighing lysimeter. Water. 17(2):187. doi: 10.3390/w17020187.

Rodell M, Famiglietti JS, Chen J, Seneviratne SI, Viterbo P, Holl S, Wilson CR. 2004. Basin scale estimates of evapotranspiration using GRACE and other observations. Geophys Res Lett. 31(20):2004GL020873. doi: 10.1029/2004GL020873.

Salazar-Martínez D, Holwerda F, Holmes TR, Yépez EA, Hain CR, Alvarado-Barrientos S, Ángeles-Pérez G, Arredondo-Moreno T, Delgado-Balbuena J, Figueroa-Espinoza B, Garatuza-Payán J. 2022. Evaluation of remote sensing-based evapotranspiration products at low-latitude eddy covariance sites. Journal of Hydrology. 610:127786. doi: 10.1016/j.jhydrol.2022.127786.

Sejine H, Anane M. 2025. Remote sensing and GIS-based WetSpass-S model for estimating actual evapotranspiration in Grombalia region, Northeast Tunisia: comparison with ETLook WaPOR model. Euro-Mediterr J Environ Integr. 10(2):949–964. doi: 10.1007/s41207-024-00628-7.

Souza VA, Roberti DR, Ruhoff AL, Zimmer T, Adamatti DS, Gonçalves L de, Diaz MB, Alves RCdCM, Moraes O de 2019. Evaluation of MOD16 algorithm over irrigated rice paddy using flux tower measurements in Southern Brazil. Water. 11(9):1911. doi: 10.3390/w11091911.

Velpuri NM, Senay GB, Singh RK, Bohms S, Verdin JP. 2013. A comprehensive evaluation of two MODIS evapotranspiration products over the conterminous United States: using point and gridded FLUXNET and water balance ET. Remote Sens Environ. 139:35–49. doi: 10.1016/j.rse.2013.07.013.

Verwey P, Vermeulen P. 2011. Influence of irrigation on the level, salinity and flow of groundwater at Vaalharts Irrigation Scheme. WSA. 37(2):155–164. doi: 10.4314/wsa.v37i2.65861.

Weerasinghe I, Bastiaanssen W, Mul M, Jia L, Van Griensven A. 2020. Can we trust remote sensing evapotranspiration products over Africa? Hydrol Earth Syst Sci. 24(3):1565–1586. doi: 10.5194/hess-24-1565-2020.

Yin J, Zhan X, Barlage M, Kumar S, Fox A, Albergel C, Hain CR, Ferraro RR, Liu J. 2023. Assimilation of blended satellite soil moisture data products to further improve noah-MP model skills. J Hydrol. 621:129596. doi: 10.1016/j.jhydrol.2023.129596.

Zhang C, Long D. 2021. Estimating spatially explicit irrigation water use based on remotely sensed evapotranspiration and modelled root zone soil moisture. Water Resour Res. 57(12):1–27. doi: 10.1029/2021WR031382.